Construction of Hyperbranched Poly(alkenephenylene)s by Diyne Polycyclotrimerization: Single-Component Catalyst, Glycogen-like Macromolecular Structure, Facile Thermal Curing, and Strong Thermolysis Resistance

Ronghua Zheng,[†] Hongchen Dong,[†] Han Peng,[†] Jacky W. Y. Lam,[†] and Ben Zhong Tang*[,†,‡]

Department of Chemistry, The Hong Kong University of Science & Technology, Clear Water Bay, Kowloon, Hong Kong, China, and Department of Polymer Science and Engineering, Peking University, Beijing 100871, China

Received January 16, 2004; Revised Manuscript Received April 29, 2004

ABSTRACT: A "simple" catalyst of $TaBr_5$, $NbBr_5$, or $NbBr_3{\cdot}CH_3O(CH_2)_2OCH_3$ is developed, which readily effects polycyclotrimerizations of α,ω-alkenediynes {HC≡C$(CH_2)_m$C≡CH, m = 4−6 [**1**(m)]} at room temperature, giving hyperbranched poly(alkenephenylene)s [*hb*-P**1**(m)] with high molecular weights (M_w up to ∼270 × 10^3) in high yields (normally >80%). The polymers prepared under optimal reaction conditions are completely soluble in common organic solvents such as toluene, THF, and chloroform. Spectroscopic characterizations prove that the polymers comprise of linear (*L*) and dendritic units (*D*) of 1,2,4/1,3,5-trialkylbenzenes and terminal unit (*T*) of 1,2,4-trialkylbenzene (or 6-alkyltetralin). The *L* and *D* units are generated by geostructurally different addition modes, similar to those used by nature to create *L* and *D* units of glycogen, a hyperbranched biopolymer. With the aids of model reactions and simulations, detailed structural analyses reveal that *hb*-P**1**(4) possesses a degree of branching of 64% and consists of 36%, 32%, and 32% of *L*, *D*, and *T* units, respectively, with 1,2,4-trialkylbenzene being the predominant isomeric structure (74%). The polymer shows outstanding thermal properties: it readily cures when baked at a moderate temperature of 100 °C and loses little of its weight when heated to a high temperature of ∼500 °C.

Introduction

Naturally occurring macromolecules with highly branched structures (or hyperbranched biopolymers) serve important biological functions in the living world. Glycogen, for example, is a polymer of glucose with a treelike structure (Chart 1) that is used by animals as solid fuels to store and transport energy.[1,2] Nature has admirably designed the molecular structure of glycogen for fulfilling its biological missions.[3] Its linear structure (*L*) enables the carbohydrate chain to be readily synthesized or degraded respectively by glycogenesis or glycogenolysis catalyzed by the enzymes abundant in the living cells, noting that most proteins are linear polymers. The dendritic structure (*D*), on the other hand, populates the terminal groups (*T*) in the three-dimensional space, allowing many glucose monomers to be added to, or released from, glycogen in parallel on demand. This ensures fast polymer synthesis or degradation and hence quick responses to physiological requests or stimuli. The geometric distribution of the *L* and *D* units in glycogen is random, which may be aesthetically unattractive but practically useful. The geostructural randomness, for example, endows the hyperbranched biopolymers with great conformational flexibilities to cope with variegated biological circumstances or situations in different species.[4,5]

As discussed above, both *L* and *D* units are indispensable for glycogen to perform its biological duties.

Chart 1

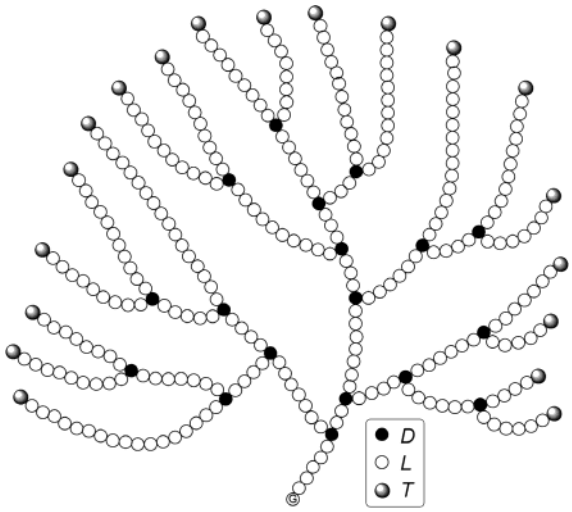

Scrutiny of the glycogen structure reveals that the *L* and *D* units are formed respectively via α-1,4 and α-1,6 glycosidic linkages (or ethereal bonds) of the glucose residues.[3] In other words, the *L* and *D* units of the hyperbranched biopolymer are generated by the linking modes that are same in chemical nature but different in geometric structure. Creation of hyperbranched synthetic polymers is a hot topic of current interest,[6−8] and many such polymers have been prepared by polymerizations of AB_m-type monomers, where A and B are mutually reacting functional groups with $m \geq 2$. In such systems, the *D* units are generated by polycoupling of A and B groups, whereas the *L* units are formed when some B groups are left unreacted inside the cores, as

[†] The Hong Kong University of Science & Technology.
[‡] Peking University.
* To whom correspondence should be addressed (The Hong Kong University of Science & Technology): phone +852-2358-7375; Fax +852-2358-1594; e-mail tangbenz@ust.hk.

10.1021/ma049871+ CCC: $27.50
Published on Web 06/11/2004

Scheme 1

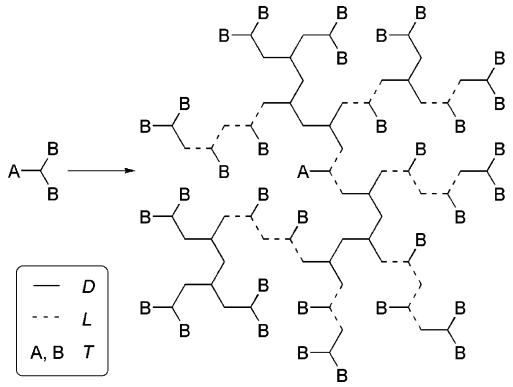

diagrammatically illustrated in Scheme 1 for an AB_2-type polycondensation. The formation of the *L* units is thus mechanistically associated with the incomplete coupling or mismatching between A and B groups, which may explain why the *L* units are often referred to as structural defects in the research community of dendritic polymers. Clearly, the biological and synthetic systems are taking different mechanistic approaches to the creation of the *L* and *D* units.

We here report a simple transition-metal-catalyzed diyne polycyclotrimerization system that generates the *L* and *D* units by a mechanism similar to that of the biological system but different from that of the "conventional" synthetic system. In the diyne polycyclotrimerization, all the triple bonds are reacted, without any unreacted ethynyl functional groups left inside the core, which thus differs our system from the traditional AB_m-type polycondensation system. The polymerization propagates in linking modes that are same in chemical nature but different in geometric structure (Scheme 2), thus sharing a mechanistic similarity to glycogenesis in the living cells. The simultaneous propagations via the different geometric growth patterns give rise to poly(alkenephenylene)s with hyperbranched structures consisting of both *L* and *D* repeat units of random distribution [*hb*-P**1**(*m*); Scheme 3]. This geostructural irregularity makes the polymers completely soluble in common organic solvents and readily processable by normal solution techniques. The high density of the aromatic rings confers strong thermolysis resistance on the polymers: *hb*-P**1**(4), for example, loses almost no weight when heated to a temperature as high as ~500 °C.

Experimental Section

Materials. Unless otherwise stated, all the solvents and reagents used in this study were purchased from Aldrich and used as received. Toluene, hexane, dioxane, and THF were distilled from sodium benzophenone ketyl immediately prior to use. Dichloromethane (DCM) was distilled over calcium hydride. Metal halides MX_5 (M = Ta, Nb; X = F, Cl, Br, I) and trihalo(1,2-dimethoxyethane)niobium [NbX'_3L: X = Cl, Br; L = $CH_3OCH_2CH_2OCH_3$ (DME)] were commercial products (Aldrich) of highest purities. 1,7-Octadiyne, 1,8-nonadiyne, and 1,9-decadiyne were purchased from Farchan, distilled from calcium hydride, and stored in a dark, cold, dry place in an exposure-proof refrigerator. Heteroatom-containing diyne [$(CH{\equiv}C\text{-}p\text{-}C_6H_4)_2Si(CH_3)_2$] and triyne [$(CH{\equiv}C\text{-}p\text{-}C_6H_4)_3N$] were synthesized in our laboratories according to our previously published procedures.[9]

Instrumentation. Weight (M_w)- and number-average molecular weights (M_n) and polydispersity indexes (PDI) of the polymers were estimated by a Waters Associates gel permeation chromatograph (GPC) system in THF using a set of monodisperse polystyrenes as calibration standards. IR spectra were recorded on a Perkin-Elmer 16 PC FTIR spectrophotometer using solid films on, or liquid films between, sodium chloride plates. ^1H and ^{13}C NMR spectra were measured on a Bruker ARX 300 NMR spectrometer using chloroform-*d* as solvent and tetramethylsilane (TMS) as internal reference (δ = 0). Mass spectra were recorded on a Finnigan TSQ 7000 triple quadrupole spectrometer operating in a chemical ionization (CI) mode using methane as carrier gas. UV−vis spectra were measured on a Milton Ray Spectronic 3000 array spectrophotometer, using DCM as solvent. Thermogravimetric analyses (TGA) were carried out on a Perkin-Elmer TGA 7 analyzer at a heating rate of 20 °C/min under nitrogen or in air.

Polymerization. All polycyclotrimerization reactions were carried out under nitrogen using standard Schlenk techniques. A typical experimental procedure for the polymerization of **1**(4)

Scheme 2

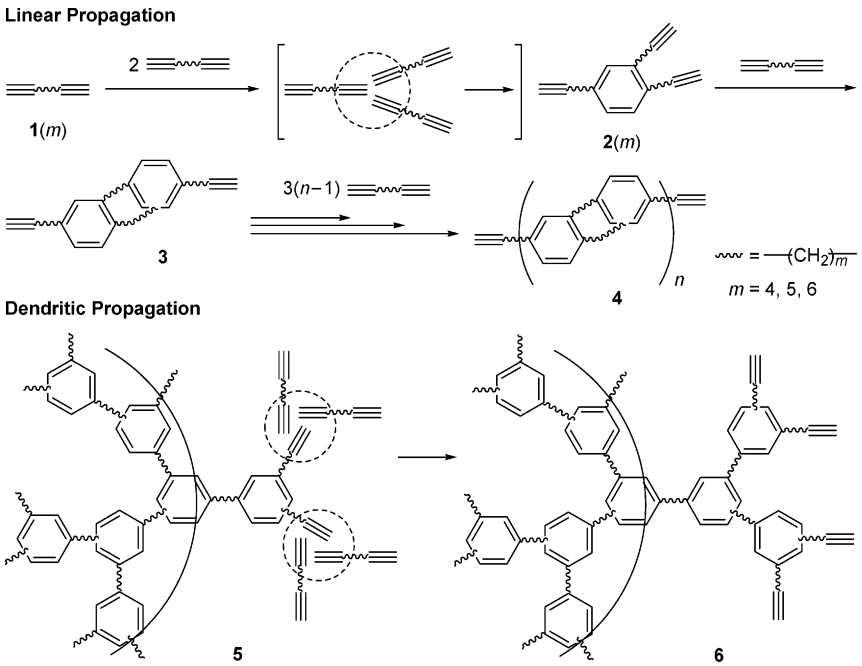

Scheme 3

Polycyclotrimerizations of Diynes [1(*m*)] Initiated by Transition-Metal Catalysts ($ML_uL'_v$)

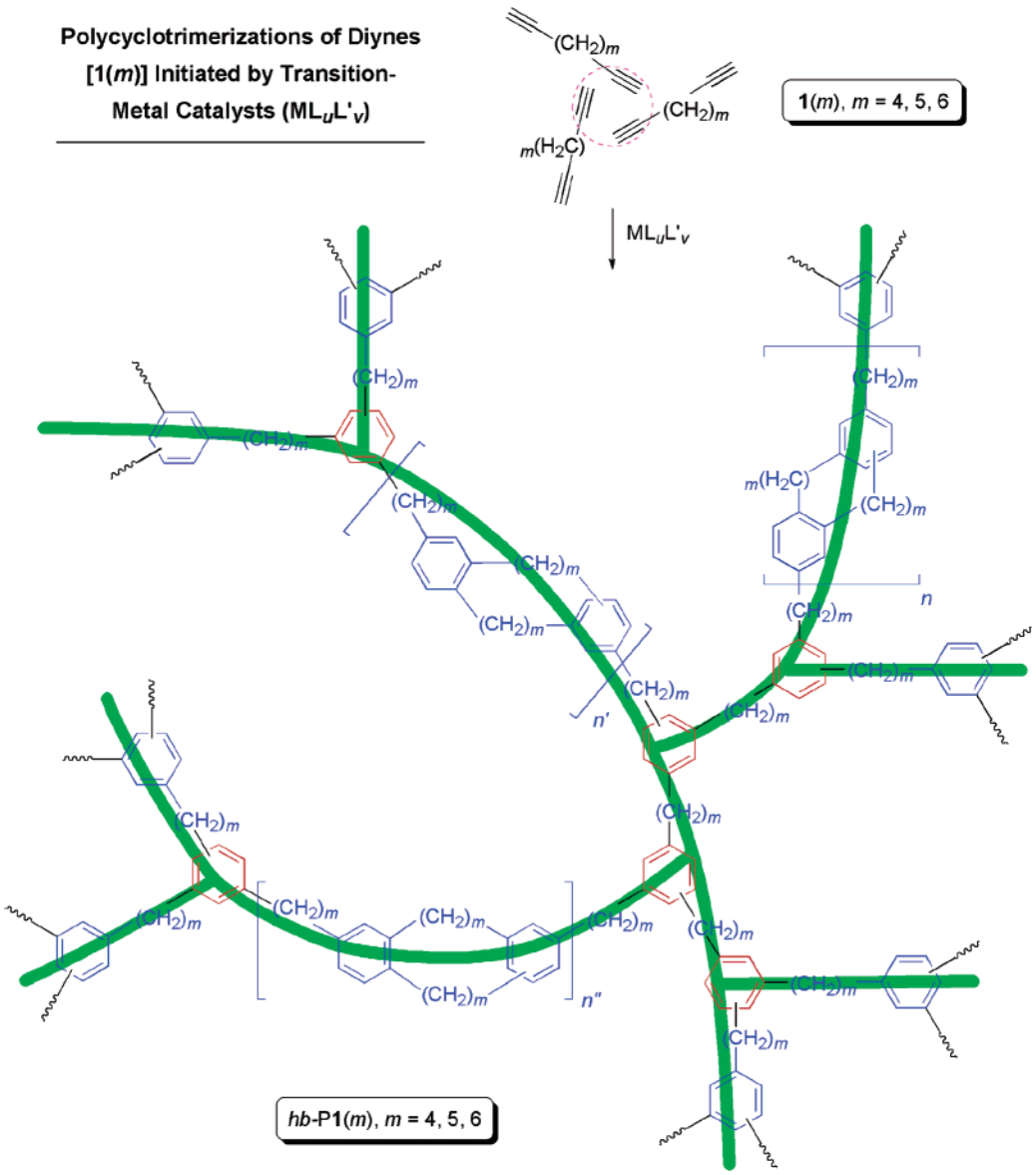

is given below as an example. To a thoroughly baked and carefully evacuated 15 mL Schlenk tube with a three-way stopcock on the sidearm was placed 14.5 mg (0.025 mmol) of $TaBr_5$ under nitrogen in a glovebox. Freshly distilled toluene (2.3 mL) was injected into the tube using a hypodermic syringe, and the mixture was stirred for 5 min. Monomer, **1**(4) (0.20 mL, 1.5 mmol) was then syringed into the catalyst solution. The resultant mixture was stirred at room temperature under nitrogen for 6 h, after which the reaction was quenched by a few drops of methanol. The mixture was added dropwise to ~300 mL of methanol through a cotton filter under stirring. The polymer precipitate was allowed to stand overnight and was then collected by filtration. The isolated polymer was washed with methanol and dried under vacuum at room temperature to a constant weight. A white powdery product of *hb*-P**1**(4) was obtained in 80%. M_w: 30 800; PDI: 3.4 (GPC). IR (thin film), ν (cm^{-1}): 3004 (Ar−H stretching), 2929 (CH_2 asymmetrical stretching), 2856 (CH_2 symmetrical stretching), 1893, 1770 (overtone band, trisubstituted benzene ring), 1602, 1575, 1500, 1460 (−C═C− ring stretching), 1456, 1438 (CH_2 scissoring), 825, 809, 755, 708 (Ar−H bending). ^{1}H NMR (300 MHz, $CDCl_3$), δ (ppm): 7.01, 6.94, 6.90, 6.86, 6.79 (Ar−H), 2.71, 2.55 (Ar−CH_2), 1.76, 1.63 (Ar−CH_2−CH_2). ^{13}C NMR (75 MHz, $CDCl_3$), δ (ppm): 142.4, 139.6, 136.7, 134.2, 128.9, 125.5 [aromatic (C_6H_3) carbons), 35.5, 31.3, 29.1, 23.4 [aliphatic (CH_2) carbons]. UV (DCM, 7.5 × 10^{-4} M), λ_{max} (nm)/ϵ_{max} (mol^{-1} L cm^{-1}): 232/2275, 269/707, 277/616.

Preparation of Model Compounds: 1,2,4- and 1,3,5-Trihexylbenzenes (8). Trisubstituted benzenes were synthesized as model compounds by monoyne(/diyne) (co)cyclizations under conditions similar to those used in the diyne polycyclotrimerization described above. For preparation of **8**, the reaction was carried out in toluene (5 mL), using 1-octyne (0.74 mL, 5.0 mmol) as reactant and $TaBr_5$ (29.0 mg, 0.05 mmol) as catalyst (Scheme 4). The reaction products were purified by silica gel chromatography, using hexane as eluent. A colorless liquid of **8** was isolated in ~91% yield. Separation of 1,2,4-**8** from 1,3,5-**8** was attempted but failed. The molar ratio of 1,2,4-**8** to 1,3,5-**8** was estimated by NMR analysis to be 3.0:1.0. IR (neat), ν (cm^{-1}): 3000 (Ar−H stretching), 2956, 2870 (CH_3 stretching), 2927, 2857 (CH_2 stretching), 1888, 1771 (overtone band, trisubstituted benzene ring), 1603, 1572, 1499 (−C═C− ring stretching), 1466 (CH_2 scissoring), 1378 (CH_3 bending), 823 (Ar−H bending), 724 (CH_2 rocking). ^{1}H NMR (300 MHz, $CDCl_3$), δ (ppm): 7.04 [d, 1H, Ar−H (g)], 6.94 [s, 1H, Ar−H (h)], 6.92 [overlapping dd, 1H, Ar−H (i)], 6.80 [s, 3H, Ar−H (j)], 2.56 (m, 6H, Ar−CH_2−), 1.56 (m, 6H, Ar−CH_2−CH_2−), 1.30 (m, 18H, −CH_2−), 0.88 (m, 9H, −CH_3). ^{13}C NMR (75 MHz, $CDCl_3$), δ (ppm): 142.7, 140.3, 140.1, 137.7, 129.2, 128.9, 125.8, 125.7 (aromatic carbons), 36.0, 35.6 (Ar−CH_2−), 31.8, 31.6, 31.4 (Ar−CH_2−CH_2), 32.8, 32.4, 29.5, 29.1, 22.7, 22.6 (−CH_2−), 14.1 (−CH_3). MS (CI): *m/e* 331.3 [$(M + 1)^+$]. UV (DCM, 7.5 × 10^{-4} mol/L), λ_{max} (nm)/ϵ_{max} (mol^{-1} L cm^{-1}): 231/1863, 269/539, 277/447.

Scheme 4

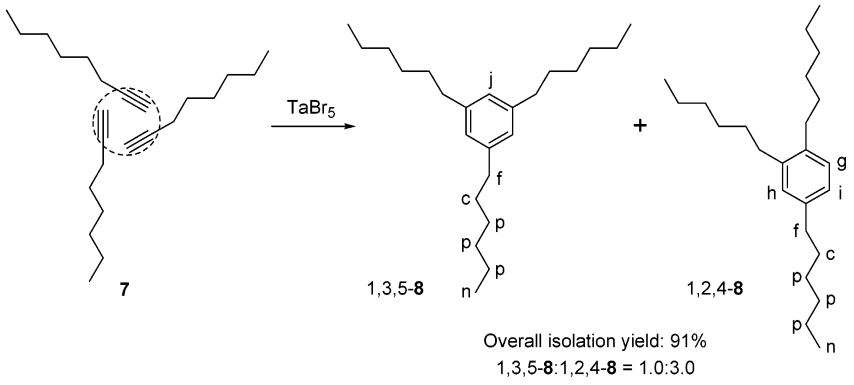

Scheme 5

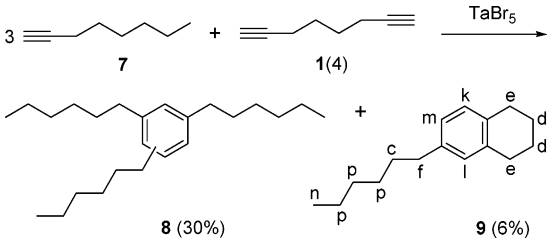

6-Hexyl-1,2,3,4-tetrahydronaphthalene or 6-Hexyltetralin (9). This model compound was prepared by the cocyclization reaction of 1,7-octadiyne (0.13 mL, 0.98 mmol) with 1-octyne (0.44 mL, 2.98 mmol) catalyzed by $TaBr_5$ (29.0 mg, 0.05 mmol) in 4.4 mL of toluene by a procedure similar to that used in the polymerization reaction (Scheme 5). The product was purified by silica gel column chromatography, using hexane as eluent. A colorless liquid of **9** was obtained in an isolation yield of 6.3%. IR (neat), ν (cm^{-1}): 3002 (Ar−H stretching), 2955, 2871 (CH_3 stretching), 2927, 2857 (CH_2 stretching), 1602, 1578, 1503 (−C═C− ring stretching), 1460 (acyclic CH_2 scissoring), 1456 (cyclic CH_2 scissoring), 1377 (CH_3 bending), 826, 807 (Ar−H bending), 727 (CH_2 rocking). ^{1}H NMR (300 MHz, $CDCl_3$), δ (ppm): 6.97 [d, 1H, Ar−H (k)], 6.90 [overlapping dd, 1H, Ar−H (m)], 6.88 [s 1H, Ar−H (l)], 2.73 (br, 4H, cyclic $-CH_2-$) 2.52 (t, 2H, acyclic $-CH_2-$), 1.78 (m, 4H, cyclic Ar−CH_2−CH_2−), 1.56 (m, 2H, acyclic Ar−CH_2−CH_2−), 1.30 (m, 6H, $-CH_2-$), 0.88 (m, 3H, $-CH_3$). ^{13}C NMR (75 MHz, $CDCl_3$), δ (ppm): 140.0, 136.8, 134.2, 129.0, 128.9, 125.6 (aromatic carbons), 35.6 (acyclic Ar−CH_2−), 31.7 (acyclic Ar−CH_2−CH_2−), 29.4, 29.0 (cyclic Ar−CH_2−), 23.3, 23.2 (cyclic Ar−CH_2−CH_2−), 31.8, 29.1, 22.6 (−CH_2−), 14.1 (−CH_3). MS (CI): *m/e* 216.2 (M^+).

Results and Discussion

Polymerization Behaviors. We have previously found that alkyne polycyclotrimerizations can be effected by $TaCl_5$−Ph_4Sn.[10,11] To prepare the binary-mixture catalyst, stoichiometric amounts of $TaCl_5$ and Ph_4Sn need to be mixed in a proper solvent and aged for an adequate period at a desired temperature with care. Compared to the binary mixture, a single-component catalyst is preferable and is particularly welcomed by industrial technologists because such a catalyst will enjoy many advantages including low cost, easy handling, and simple operation. In this work, we explored the possibility of using the metal halides alone to initiate the alkyne polycyclotrimerizations in the absence of secondary components of "cocatalysts", with the aim of developing simple, monocomponent catalyst systems.

We first attempted to polycyclotrimerize 1,7-octadiyne [**1**(4)] by tantalum halides, and the results are summarized in Table 1. TaF_5 catalyzes the polycyclotrimerization of **1**(4) in a sluggish way, producing little amount of polymer (3%) after 7 h reaction. As mentioned above, the $TaCl_5$−Ph_4Sn mixture is a good catalyst for the diyne polycyclotrimerization, but $TaCl_5$ alone affords a polymeric product that is only partially soluble in common solvents (Table 1, run 2).[12] Delightfully, $TaBr_5$ effectively catalyzes the polycyclotrimerization of **1**(4), giving a completely soluble polymer in a high yield (81%). The excellent solubility of the polymer allows its molecular weights to be estimated by GPC, whose M_w is found to be as high as 55 300. (The absolute M_w of the polymer is probably much higher than this relative value calibrated by the linear polystyrene standards because it is well-known that the GPC analyses often underestimate the molecular weights of hyperbranched polymers.[10,13]) TaI_5 is, however, practically incapable of initiating the diyne polycyclotrimerization. Clearly, the catalytic activity of the tantalum halide is dramatically affected by its halogen anion, with $TaBr_5$ being the best catalyst for the diyne polycyclotrimerization. Too tight or loose binding of the too small (F^-) or big halogen anion (I^-) with the transition-metal center is not good—the halogen anion with the "right" bonding force or atomic size (Br^-) showing the best performance as the polycyclotrimerization catalyst.

Similar but more pronounced halogen effects are observed in the case of niobium halides: the bromide gives a soluble polymer of high molecular weight (Table 1, run 7) and the chloride yields only partially soluble polymer, whereas the fluoride and the iodide completely fail to initiate the diyne polymerization. Overall, the catalytic activities of the niobium halides are lower than those of their tantalum counterparts, suggesting that the metal center also plays an important role in

Table 1. Polymerization of 1,7-Octadiyne 1(4)[a]

run	catalyst	yield (%)	S[b]	M_w[c]	PDI[c]
1	TaF_5	3			
2	$TaCl_5$	76	△		
3	$TaBr_5$	81	√	55 300	4.7
4	TaI_5	*d*			
5	NbF_5	0			
6	$NbCl_5$	58	△		
7	$NbBr_5$	49	√	20 900	3.4
8	NbI_5	0			
9	$NbCl_3$·DME[e]	79	√	95 500	6.5
10	$NbBr_3$·DME[e]	0			

[a] Carried out in toluene under nitrogen at room temperature for 7 h; $[M]_0 = 0.6$ M, [cat.] = 20 mM (40 mM for run 9). [b] Solubility (S) tested in common organic solvents such as THF, toluene, DCM, and chloroform: △ = partially soluble; √ = completely soluble. [c] Measured by GPC in THF on the basis of a polystyrene calibration. [d] Trace amount. [e] DME = 1,2-dimethoxyethane.

Table 2. Polymerizations of Di- and Triynes in the Presence of $TaBr_5$[a]

run	monomer	$[M]_0$ (M)	yield (%)	S[b]	M_w[c]	PDI[c]
1	1,7-octadiyne [**1**(4)]	0.60	80	√	30 800	3.4
2	1,8-nonadiyne [**1**(5)]	0.27	80	√	206 400	6.2
3	1,9-decadiyne [**1**(6)]	0.24	83	√	268 500	6.1
4	$(CH{\equiv}C\text{-}p\text{-}C_6H_4)_2Si(CH_3)_2$	0.10	61	√	48 600	3.2
5	$(CH{\equiv}C\text{-}p\text{-}C_6H_4)_3N$	0.10	90	×		

[a] Carried out under nitrogen in toluene at room temperature for 6 h. For runs 1−3, $[TaBr_5] = 10$ mM; for runs 4 and 5, $[TaBr_5] = 5$ mM. [b] Solubility (S) tested in common organic solvent such as THF, toluene, DCM, and chloroform: √ = completely soluble; × = insoluble. [c] Measured by GPC in THF on the basis of a polystyrene calibration.

determining the catalytic activity of the metal halide. When a niobium chloride complex with a 1,2-dimethoxyethane ligand ($NbCl_3$·DME) is used to initiate the polycyclotrimerization, excellent catalytic activity is observed: a high molecular weight polymer is obtained in a high yield (Table 1, run 9). In sharp contrast, its bromide congener ($NbBr_3$·DME) cannot catalyze the diyne polymerization at all.[14] This set of experimental data, coupled with the halogen effects discussed above, clearly indicates that the catalytic activity of the transition-metal halide can be greatly tuned by molecular engineering of halogen anion or organic ligand. We are currently working on the development of new catalysts with superior catalytic performance through ligand coordination chemistry,[15,16] and the results will be published in a separate paper in due course.

After identifying that $TaBr_5$ was an excellent catalyst for the polycyclotrimerization of **1**(4), we tried to use it to polycyclotrimerize other diyne and triyne monomers. As can be seen from Table 2, $TaBr_5$ can effectively catalyze the polycyclotrimerizations of all the three alkenediynes tested in this study, that is, **1**(4), **1**(5), and **1**(6), giving hyperbranched poly(alkenephenylene)s with high molecular weights (M_w up to $\sim 270 \times 10^3$) in high yields (≥80%). $TaBr_5$ can also initiate polycyclotrimerizations of heteroatom-containing arylenediynes.[10,11] The polycyclotrimerization of a silicon-containing diyne, namely, bis(4-ethynylphenyl)dimethylsilane, proceeds smoothly at low catalyst and monomer concentrations, resulting in the formation of a completely soluble polymer. These results clearly prove that $TaBr_5$ is an excellent catalyst for diyne polycyclotrimerizations. Triynes can also be polycyclotrimerized by $TaBr_5$, but the resultant polymers are often insoluble: for example, the polymerization of tris(4-ethynylphenyl)amine catalyzed by $TaBr_5$ proceeds rapidly, and the polymerization solution quickly gels (Table 2, run 5). The triynes can be polymerized into soluble polymers through their copolycyclotrimerizations with di- and/or monoynes, which will be the subject of our next publication.[17]

Using **1**(4) as a model monomer, we systematically studied the effects of reaction conditions on the alkyne polycyclotrimerization in an effort to understand the polymerization behaviors and to optimize the polymerization process. Figure 1A shows the effect of initial monomer concentration ($[M]_0$) on the polycyclotrimerization of **1**(4). When $[M]_0$ is lower than 0.30 M, the polymerization is sluggish: the isolation yields of the polymers and their molecular weights are both low, being ∼3% and $\leq 10 \times 10^3$, respectively. Increasing $[M]_0$ to 0.6 M dramatically increases the polymer yield (80%) and molecular weight ($M_w \sim 30 \times 10^3$). But if $[M]_0$ is

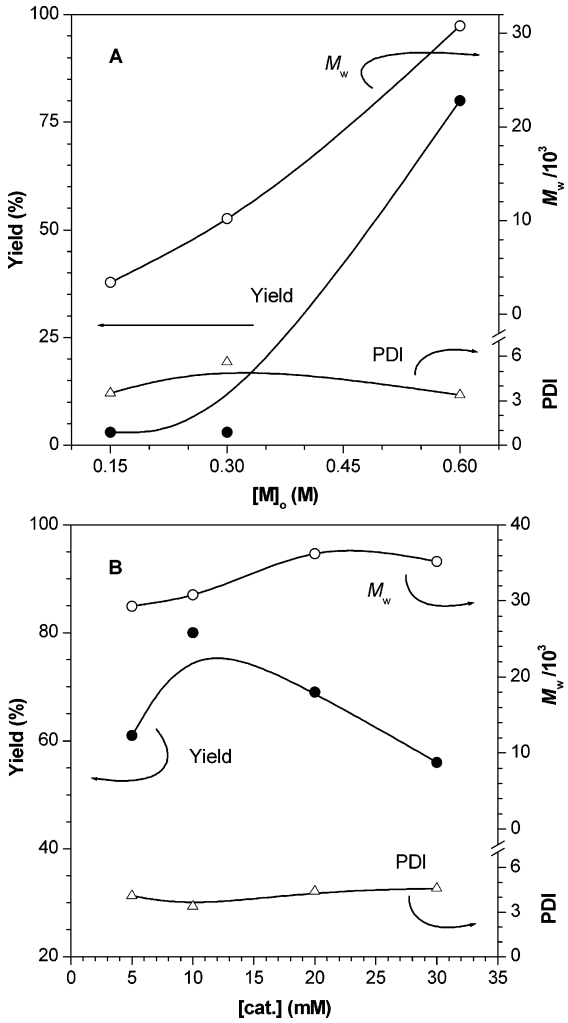

Figure 1. Effects of concentrations of (A) monomer and (B) catalyst on the polycyclotrimerizations of 1,7-octadiyne [**1**(4)] catalyzed by $TaBr_5$ in toluene at room temperature for 6 h; for (A), [cat.] = 10 mM; for (B), $[M]_0 = 0.6$ M.

further increased to beyond 0.90 M, the polymerization becomes too vigorous to control; as a result, the resultant polymers become only partially soluble. There exists a monomer concentration window, with the optimal $[M]_0$ being ∼0.60 M. This concentration effect is understandable because at too low $[M]_0$, the polymerization reaction will be actively terminated by the intramolecular cyclization of the propagating species with the diyne molecules (vide post), whereas at too high $[M]_0$, intermolecular reactions between the propagating species will lead to the formation of cross-linking networks.

Compared to $[M]_0$, the catalyst concentration [cat.] has less effect on the polycyclotrimerization of **1**(4) (Figure 1B). Whereas doubling $[M]_0$ (from 0.3 to 0.6 M) can greatly accelerate the polymerization (cf. Figure 1A), increasing [cat.] by 6-fold (from 5 to 30 mM) does not cause as much change. The isolation yields and molecular weights of all the polymers are high in the whole range of catalyst concentrations, with [cat.] of 10 mM being the best when the polymer yield is concerned. All the isolated polymeric products are completely soluble in common organic solvents such as toluene, benzene, THF, dioxane, DCM, and chloroform.

Table 3 shows the effect of solvent on the polycyclotrimerization of **1**(4). The solvent strongly affects the diyne polymerization. In the electron-donating solvents

Table 3. Solvent Effect on Polymerization of 1,7-Octadiyne 1(4)[a]

run	solvent	yield (%)	S[b]	M_w[c]	PDI[c]
1	THF	0			
2	dioxane	0			
3	DCM	31	√	27 800	3.0
4	toluene	80	√	30 800	3.4
5	hexane	10	△		

[a] Carried out at room temperature under nitrogen for 6 h using $TaBr_5$ as catalyst; [cat.] = 10 mM, $[M]_0$ = 0.60 M. [b] Solubility (S) tested in common organic solvents such as THF, toluene, DCM, and chloroform: √ = completely soluble; △ = partially soluble. [c] Measured by GPC in THF on the basis of a polystyrene calibration.

of THF and dioxane, the polymerization of **1**(4) is completely inhibited. The electron-rich solvent molecules may have coordinately complexed with the electron-deficient transition-metal center and have thus deactivated the metal halide catalyst. The polymerization occurs in a less polar solvent of DCM, but the polymer yield is low (31%). In a nonpolar solvent of toluene, the diyne polycyclotrimerization propagates smoothly, resulting in the formation of a polymer with a high molecular weight in a high yield (Table 3, run 4). Hexane is also a nonpolar solvent, but it does not perform well as a solvent for the polycyclotrimerization of **1**(4): the yield is low (10%), and the polymer is only partially soluble. This is probably due to the precipitation of high molecular weight polymers at the early stage of the polycyclotrimerization reaction as well as the partial cross-linking of the closely located propagating species in the polymer precipitates. Among all the solvents tested, toluene gives the best polycyclotrimerization results and has thus been the choice of polymerization solvent in our further investigations.

In the discussion above, we have assumed that high molecular weight polymers are formed at the early stage of the polycyclotrimerization reaction of **1**(4). To check whether this is indeed the case, we followed the time course of the polymerization reaction. As can be seen from Figure 2A, the reaction is really fast: a high molecular weight polymer is formed in a high yield in 0.5 h, the shortest time at which we stopped a polymerization reaction and collected a sample for analysis. This obviously differentiates the alkyne polycyclotrimerization from the AB_m-type polycondensation: the former is a chain polymerization while the latter is a step polymerization. Prolonging the polymerization time of **1**(4) does not help increase the polymer yield. The M_w and PDI of the polymer change little in the wide time span of 0.5−8 h.

We also investigated the influence of temperature on the polymerization of **1**(4) (Figure 2B). When the reaction temperature is increased from 0 to 90 °C, the yield of the polymer is decreased from 100% (data not shown) to 49%. The polymer formed at 0 °C is insoluble because the very fast polymerization at the low temperature makes the reaction difficult to control. All of the polymers obtained from the polymerizations carried out at other temperatures are, however, completely soluble. High temperature is not good to the diyne polycyclotrimerization because both molecular weight and polydispersity index of the polymer decrease with an increase in the temperature. Room temperature (~23 °C) is used in most of the polymerization reactions conducted in this work because the room temperature reactions can afford high molecular weight polymers with excellent solubility in high yields.

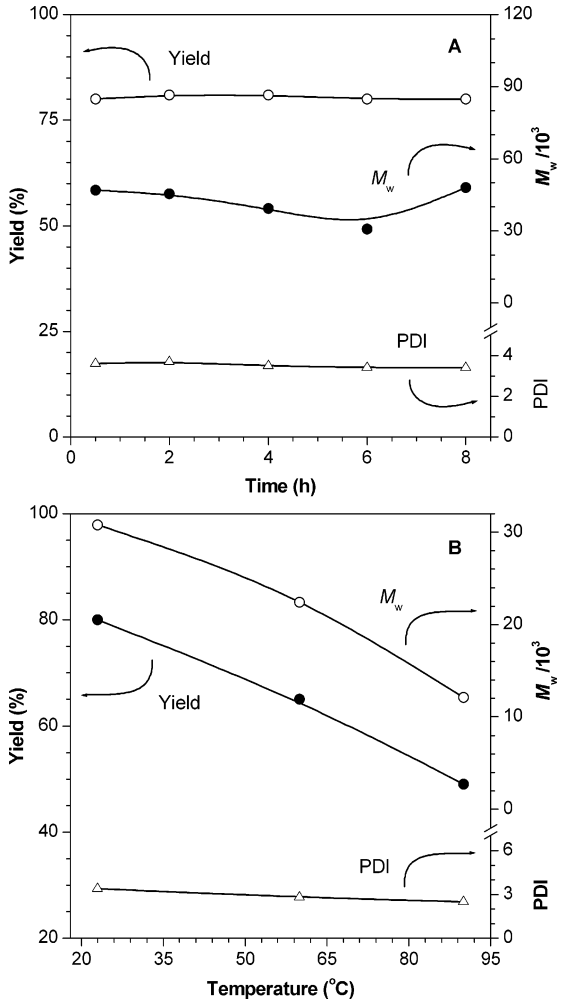

Figure 2. (A) Time course of, and (B) temperature effect on, the polymerizations of 1,7-octadiyne **1**(4) ($[M]_0$ = 0.6 M) catalyzed by $TaBr_5$ (10 mM) in toluene; for (A), at room temperature; for (B), for 6 h.

Structural Characterization. In the polymerization reactions described above, we used $TaBr_5$ as a single-component replacement for the binary mixture of $TaCl_5$−Ph_4Sn, with the belief that the $TaBr_5$-catalyzed polymerizations propagate in the same reaction mechanism, namely, polycyclotrimerization. To make sure that $TaBr_5$ has indeed catalyzed alkyne cyclization, we carried out a model reaction of 1-octyne, a monoyne (cf. Scheme 4). Under the reaction conditions similar to those used in the diyne polymerization, the monoyne is cyclotrimerized quantitatively (or in 100% conversion), although the isolation yield of the trihexylbenzenes (**8**) is lower (~91%) due to the operational loses incurred during the product purification processes. This model reaction clearly rules out the possibility that a terminal alkyne may be polymerized by $TaBr_5$ into a linear polyene with an alternative double-bond backbone via a metathesis mechanism.[18,19] We tried to separate the 1,3,5- and 1,2,4-isomers of the cyclotrimerization product **8** by column chromatography and distillation under controlled pressures but failed to achieve our goal. Spectroscopic methods are thus used to evaluate the molar ratio of the isomers, and it is found that 1,2,4-**8** is the major product of the cyclotrimerization reaction (vide infra).

The model reaction evidently proves that the $TaBr_5$-catalyzed cyclotrimerization has converted **1**(4) into a

hyperbranched poly(alkenephenylene) or *hb*-P**1**(4). To further verify the polycyclotrimerization mechanism and to learn more about the molecular structure of *hb*-P**1**(4), we measured its spectroscopic data. Figure S1 shows IR spectra of *hb*-P**1**(4) and its monomer (Supporting Information). Monomer **1**(4) absorbs strongly at 3298 and 2117 cm^{-1} due to ≡C−H and C≡C stretching vibrations, respectively. These absorption bands completely disappear in the spectrum of *hb*-P**1**(4) (Figure S1B). Alternatively, new absorption bands appear at 1602 and 1500 cm^{-1} due to the skeletal vibrations of benzene rings.[20] These results suggest that the ethynyl groups of **1**(4) have been converted to the benzene rings of *hb*-P**1**(4) by the $TaBr_5$-catalyzed alkyne polycyclotrimerization.

The molecular structure of *hb*-P**1**(4) is further investigated by UV analysis. Figure S2 shows the UV absorption spectrum of *hb*-P**1**(4), along with those of its monomer [**1**(4)] and model compound (**8**) (Supporting Information). The spectrum of **1**(4) is a flat line parallel to the abscissa with no absorption signals recorded in the whole spectral region of 200−900 nm because its isolated acetylenic triple bonds are known to absorb at <200 nm.[20] Polymer *hb*-P**1**(4), however, absorbs in the UV region, giving three peaks at 232, 269, and 277 nm, with respective molar absorptivities of 2275, 707, and 616 mol^{-1} L cm^{-1}. All these three absorption peaks are associated with $\pi \rightarrow \pi^*$ transitions of the isolated trisubstituted benzene rings, with the peak at 232 nm assignable to the E_2 band and those at 269 and 277 nm to the B bands.[20] The absorption spectrum of model compound **8**, a mixture of 1,2,4- and 1,3,5-trihexylbenzenes, is similar to that of *hb*-P**1**(4), further supporting that the repeat units of the polymer is comprised of trialkylbenzenes, with the benzene rings separated or isolated by the nonconjugating alkyl spacers.

NMR spectroscopy is the most powerful technique for structural characterization, and indeed the NMR spectra of *hb*-P**1**(4) are very informative. Comparing the ^{1}H NMR spectrum of **1**(4) with that of *hb*-P**1**(4) shown respectively in panels A and B of Figure 3, it is clear that the resonance peaks of the ethynyl (a) and propargyl protons (b) of **1**(4) at δ 1.97 and 2.23 have disappeared after polymerization, with its resonance peak at δ 1.63 (c) being the only one left. Several new peaks appear at $\delta \sim 6.50-7.20$, 2.71, 2.55, and 1.76 in the NMR spectrum of the polymer. Model compound **8** gives resonance peaks of phenyl and benzyl protons at $\delta \sim 6.8-7.0$ (g−j) and 2.56 (f; Figure 3C), which helps assign the peaks of the polymer at $\delta \sim 6.50-7.20$ and 2.55 respectively to the proton absorptions of the phenyl and benzyl groups formed by the alkyne polycyclotrimerization.

What are the peaks at δ 2.71 (e) and 1.76 (d) in the NMR spectrum of *hb*-P**1**(4) responsible for? They are probably arising from the absorptions of the methylene protons of the 1,2,3,4-tetrahydronaphthalene (or tetralin) rings formed by an end-capping dimerization reaction (vide infra). To substantiate these peak assignments, we designed another model reaction (cf. Scheme 5) and synthesized another model compound, 6-hexyltetralin (**9**). From Figure 1, we have learned that the alkyne polycyclotrimerization is sensitively affected by monomer concentration: at low $[M]_0$ (≤0.3 M), little polymer has been formed. It is therefore possible to prepare the model compound **9** using a low concentration of **1**(4) (e.g., at $[M]_0$ = 0.2 M), at which the intramolecular cyclization of the diyne molecules is favored. An excess amount of monoyne **7** (0.6 M) is added to the reaction mixture as a cautionary measure to suppress the formation of oligomeric species. Although homo- and cocyclizations of diyne **1**(4) and monoyne **7** can give many different kinds of cyclic products, it is anticipated that **9** will be formed as one of the products. Indeed, pure form of **9** can be isolated, albeit in a low yield (6%). The protons of the cyclic methylene groups show, as expected, resonance peaks at δ 2.73 (e) and 1.78 (d; Figure 3D), validating our assumption that there exist terminal units of tetralin rings in the molecular structure of the polymer.

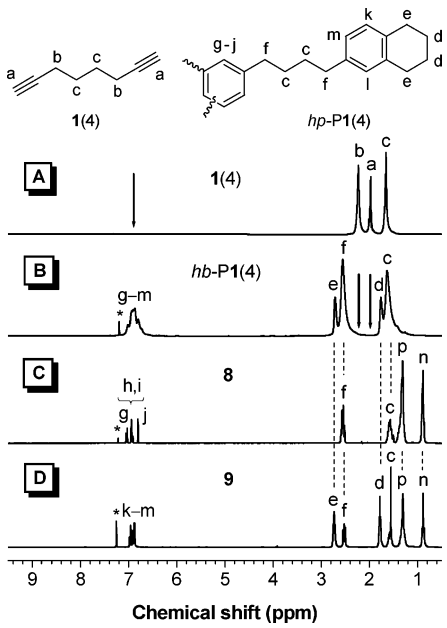

Figure 3. ^{1}H NMR spectra of chloroform-*d* solutions of (A) 1,7-octadiyne **1**(4), (B) hyperbranched polymer *hb*-P**1**(4) (sample taken from Table 3, no. 4), (C) 1,2,4/1,3,5-trihexylbenzenes **8**, and (D) 6-hexyltetralin **9**. The solvent peaks are marked with asterisks (∗).

The ^{13}C NMR spectrum of *hb*-P**1**(4) exhibits resonance peaks well corresponding to its expected molecular structure, with no any peaks unassignable. As shown in Figure 4, the resonance peaks of the ethynyl carbon atoms at δ 68.5 and 83.8 seen in the spectrum of the monomer (panel A) are absent in spectrum of the polymer (panel B). The new resonance peaks of the polymer in the aromatic ($\delta \sim 142-126$) and aliphatic regions ($\delta \sim 36-23$) can be readily identified by comparison with those of model compounds **8** and **9** (panels C and D, respectively) in the corresponding spectral regions. Summarizing the spectral data of the IR, UV, and NMR analyses, it can be concluded beyond doubt that the diyne molecules have been polymerized into hyperbranched poly(alkenephenylene)s via a polycyclotrimerization mechanism.

TGA analyses reveal that *hb*-P**1**(4) is resistant to thermolysis: a 10% weight loss is recorded when it is heated to 493 °C under nitrogen or to 465 °C in air (Figure 5). Poly(1-hexyne) $\{-[HC{=}C(C_4H_9)]_n-\}$, a linear polyalkyne with an alternative double-bond backbone, loses a similar amount of weight at ∼220 °C under nitrogen,[21] whereas linear poly(*p*-phenylene) $[-(C_6H_4)_n-]$ is stable at ∼450 °C in air or at ∼550 °C in inert atmosphere.[22] The thermal stability of *hb*-P**1**(4) is thus similar to that of the polyphenylene but different from that of the polyalkyne. This stability data serve as a

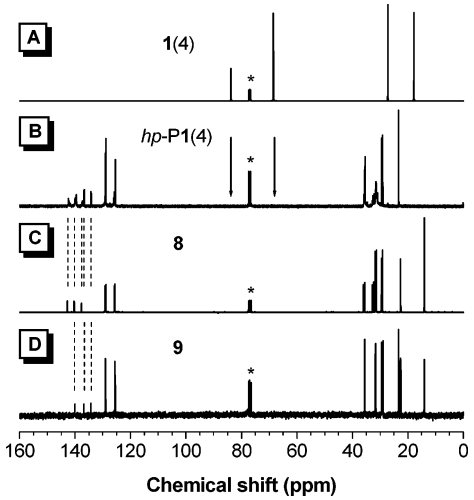

Figure 4. ^{13}C NMR spectra of chloroform-*d* solutions of (A) 1,7-octadiyne **1**(4), (B) hyperbranched polymer *hb*-P**1**(4) (sample taken from Table 3, no. 4), (C) 1,2,4/1,3,5-trihexylbenzenes **8**, and (D) 6-hexyltetralin **9**. The solvent peaks are marked with asterisks (∗).

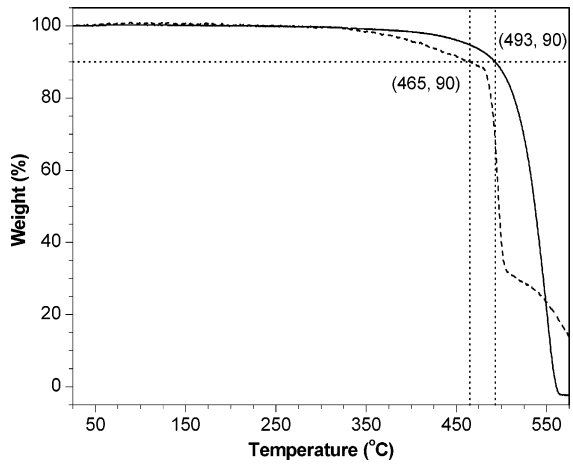

Figure 5. TGA thermograms of hyperbranched polymer *hb*-P**1**(4) (sample taken from Table 3, no. 4) recorded under nitrogen (solid line) and in air (dashed line) at a heating rate of 20 °C/min.

collateral evidence to support the conclusion derived from the spectroscopic analysis data that *hb*-P**1**(4) has a polyarylene structure. Clearly, the high thermal stability of *hb*-P**1**(4) stems from its phenylene units. Interestingly and usefully, *hb*-P**1**(4) readily cures when it is heated to a moderate temperature. The polymer remains completely soluble when warmed to 80 °C but becomes insoluble when heated to 100 °C. Baking the polymer at 100 °C for 5 h in air or under nitrogen causes it to cross-link in 95 or 96% gelation yields, and heating the polymer to 200 °C quantitatively converts it to a thermoset network. The thermal curing mechanisms of the polymer are unclear at present but may be associated with its benzyl units. Thermally activated hydrogen abstractions from the benzyl sites of *hb*-P**1**(4) may have generated numerous radical species in the macromolecular branches, the coupling of which may have facially cross-linked the polymer.

It is well-known that transition-metal-catalyzed alkyne cyclotrimerizations give rise to the formation of 1,2,4- and 1,3,5-trisubstituted benzenes, with the 1,2,4-isomers being normally the major products.[23,24] After confirming that **1**(4) has undergone polycyclotrimerization, the next issue we need to tackle is the geoisomeric structures of the repeat units of the trialkylbenzenes in the resultant polymer. Integration of ^{1}H NMR peak area has been commonly used for quantitative analysis,[20] but as can be seen from Figure 3B, the "peaks" of the polymer in the aromatic spectral region ($\delta \sim 6.50-7.20$) seem to be hopelessly complex due to severe overlapping of the resonance signals of the isomeric protons of the 1,2,4/1,3,5-trisubstituted benzenes. With the aid of model compounds **8** and **9**, we can, however, deconvolute the broad peaks of the polymer. The expanded ^{1}H NMR spectrum of **8** in the aromatic region is shown in Figure 6B, from which the peaks associated with the absorptions of the phenyl protons of 1,2,4- and 1,3,5-trihexylbenzenes can be unambiguously identified.[20,25] Using eq 1, it is calculated that molar ratio of 1,3,5-**8** to 1,2,4-**8** is 1.0:3.0 (cf. Scheme 4), in agreement with the general trends[23,24] and also with our previous experimental results;[10,11] i.e., 1,2,4-geoisomers are the major products of transition-metal-catalyzed alkyne (poly)cyclotrimerizations:

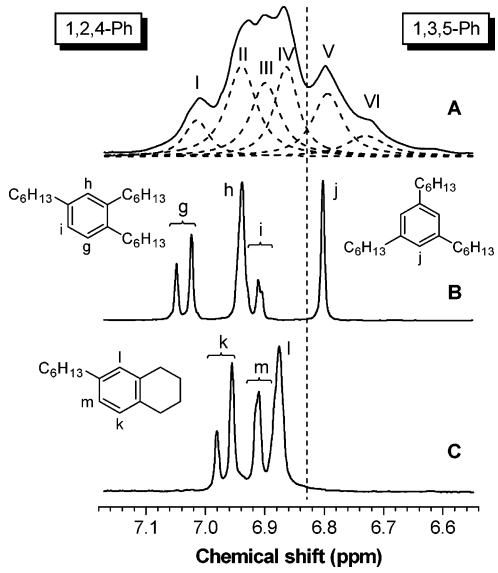

Figure 6. Expanded ^{1}H NMR spectra of (A) hyperbranched polymer *hb*-P**1**(4) (sample taken from Table 3, no. 4), (B) 1,2,4/1,3,5-trihexylbenzenes **8**, and (C) 6-hexyltetralin **9** in the chemical shift region of δ 6.54−7.18. The overlapping peaks are deconvoluted by a multipeak Lorentzian fit.

$$\frac{N_{1,2,4-\mathbf{8}}}{N_{1,3,5-\mathbf{8}}} = \frac{A_j/3}{(A_g + A_h + A_i)/3} = \frac{A_j}{A_g + A_h + A_i} \quad (1)$$

where A_j, A_g, A_h, and A_i are the integrated areas of the resonance peaks of protons j, g, h, and i of 1,3,5- and 1,2,4-**8**, respectively. The expanded ^{1}H NMR spectrum of **9** in the aromatic region can also be elucidated with ease, as clearly marked in Figure 6C. The spectral data of **9** further confirm that the aromatic protons of 1,2,4-isomers always show resonance peaks in the downfield chemical shift region ($\delta > 6.82$), in comparison to their counterparts of 1,3,5-isomers.[20,25]

The spectrum of *hb*-P**1**(4) in the aromatic region is evidently more complicated than those of model compounds **8** and **9**. The overlapping peaks of the polymer can, however, be deconvoluted or fitted by a Lorentzian function into six peaks of different intensities (given in the parentheses): δ_I 7.01 (0.17), δ_{II} 6.94 (0.54), δ_{III} 6.90 (0.42), δ_{IV} 6.86 (0.42), δ_V 6.79 (0.38), and δ_{VI} 6.73 (0.17),

Chart 2

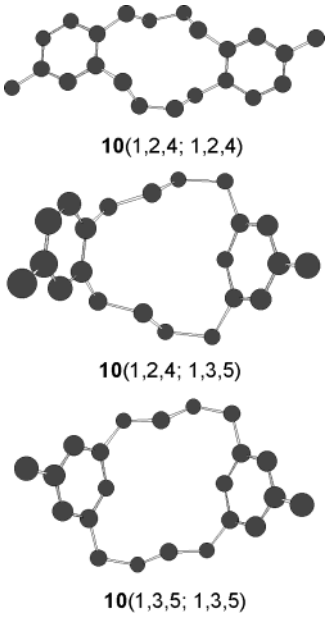

as shown in Figure 6A. From the above discussions on the peak identifications of **8** and **9** (cf. panels B and C of Figure 6), we can assign with confidence that the peaks of *hb*-P**1**(4) located in the downfield with chemical shifts of $\delta > 6.825$ on the left side of the dotted vertical line, i.e., peaks I−IV, are associated with the absorptions of the phenyl protons of the 1,2,4-isomers of the polymer, whereas those in the upfield with $\delta < 6.825$, i.e., peaks V and VI, are related to the absorptions of the phenyl protons of its 1,3,5-isomeric units. This peak differentiation enables estimation of molar ratio of the 1,2,4- and 1,3,5-isomers, $N_{1,2,4-\mathrm{Ph}}/N_{1,3,5-\mathrm{Ph}}$, by peak area integration using eq 2:

$$\frac{N_{1,2,4-\mathrm{Ph}}}{N_{1,3,5-\mathrm{Ph}}} = \frac{A_t - (A_V + A_{VI})}{A_V + A_{VI}} \qquad (2)$$

where $N_{1,2,4-\mathrm{Ph}}$ is the number of 1,2,4-substituted benzene rings, $N_{1,3,5-\mathrm{Ph}}$ the number of 1,3,5-substituted benzene rings, A_t the total integrated area of resonance peaks of all aromatic protons, A_V the integrated area of peak V at δ 6.79, and A_{VI} the integrated area of peak VI at δ 6.73. The calculated value of $N_{1,2,4-\mathrm{Ph}}/N_{1,3,5-\mathrm{Ph}}$ is 2.8, close to the value (3.0) for the model reaction of monoyne cyclization (cf. Scheme 4). This is reasonable because one may not expect that the cyclotrimerization of **1**(4), a diyne with two triple bonds separated by a flexible alkyl spacer, would differ much from that of the monoyne.[23] This agreement in the molar ratios also supports the validity of the peak deconvolution and elucidation processes.

Further detailed assignments of the individual peaks (I−VI) generated by the Lorentzian multipeak fit may be done but are not attempted because of our cautions in trying not to mislabel the peaks. Different from the isolated small molecules of the model compounds, the hyperbranched polymer is in a much more complex macromolecular environment, where not only the geometric structures of 1,2,4- and 1,3,5-isomers but also the diad sequences of different geoisomeric combinations will affect chemical shifts of the aromatic protons.[26] Chart 2 shows a few examples of simplified diad sequences, in which the different combinations of the 1,2,4- and 1,3,5-geoisomeric structures are indicated in the parentheses. Diad **10**(1,2,4; 1,2,4) has the highest probability to form from the viewpoint of reaction mechanism,[23,24] but diad **10**(1,3,5; 1,3,5) has the lowest steric energy, as revealed by the calculations using the built-in programs in the CS ChemBats3D Ultra of Cambridge Soft. It is recognized that the individual peaks may not be assigned to the particular molecular structures with confidence, unless all the diad models are synthesized and isolated in pure forms. It is, however, also noted that the preparation and purification of these model compounds, especially **10**(1,3,5; 1,3,5), are real synthetic challenges. We are now taking the challenges in our laboratories, with the aim of unambiguously assigning all the individual peaks.

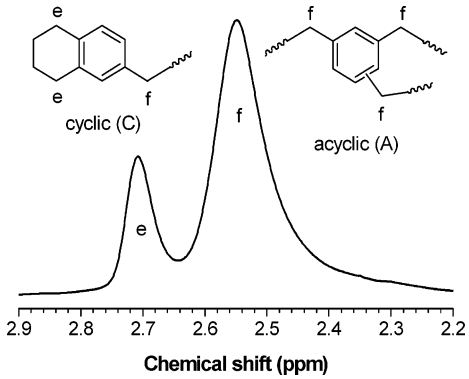

Figure 7. Expanded ^{1}H NMR spectra of hyperbranched polymer *hb*-P**1**(4) (sample taken from Table 3, no. 4) in the chemical shift region of δ 2.2−3.9.

In *hb*-P**1**(4), there exist two types of benzyl structures: one is a cyclic (C) 6-substituted tetralin type, and another is an acyclic (A) trisubstituted benzene type, as shown in Figure 7. What is the ratio of the two ($R_{C/A}$)? Knowing the ratio will help understand the polycyclotrimerization mechanisms because the formation of the tetralin-type cyclic structure terminates the growth of the propagating species. The somewhat overlapped peaks of *hb*-P**1**(4) at δ 2.71 (e) and 2.55 (f) are readily deconvoluted by a multipeak fitting function, the integration of which finds that the areas of peaks e (A_e) and f (A_f) are 0.77 and 2.81, respectively. Peak e at δ 2.71 is clearly associated with absorptions of four (4) protons of tetralin-type structure C, whereas peak f at δ 2.55 is related to the absorptions of two (2) protons of structure C and six (6) protons of structure A. The $R_{C/A}$ value can thus be calculated by eq 3:

$$R_{C/A} = \frac{A_e/4}{[A_f - (A_e/4) \times 2]/6} = \frac{3A_e}{2A_f - A_e} \qquad (3)$$

Putting the integrated areas of peaks e ($A_e = 0.77$) and f ($A_f = 2.81$) into above equation gives an experimental $R_{C/A}$ value of 0.48 (or 48%).

Mechanistic Discussion. It has become clear that the diynes have undergone polycyclotrimerizations in the presence of the transition-metal catalysts. Let us discuss how the polymerization propagates. If the propagating species grows exclusively in a linear mode, the diyne molecules will be knitted into a linear chain (**4**), but if the propagation is exclusively in a dendritic mode, a dendritic sphere (**6**) will be formed (cf. Scheme 2). In either case, the resultant polymer should bear triple bonds at the chain ends or on the sphere peripheries. None of the spectroscopic analyses have, however,

Scheme 6

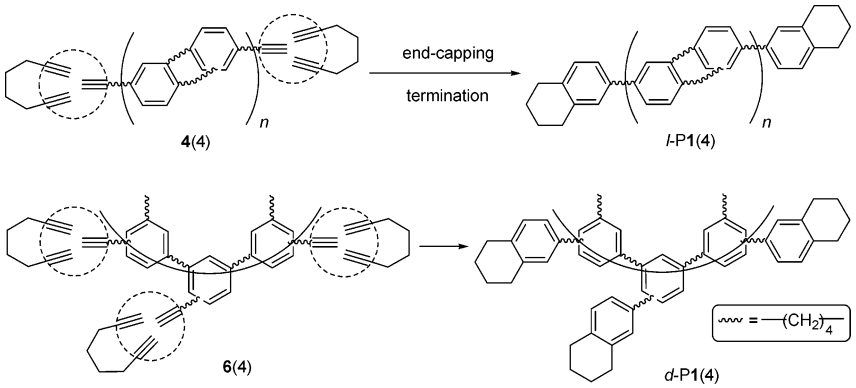

Chart 3

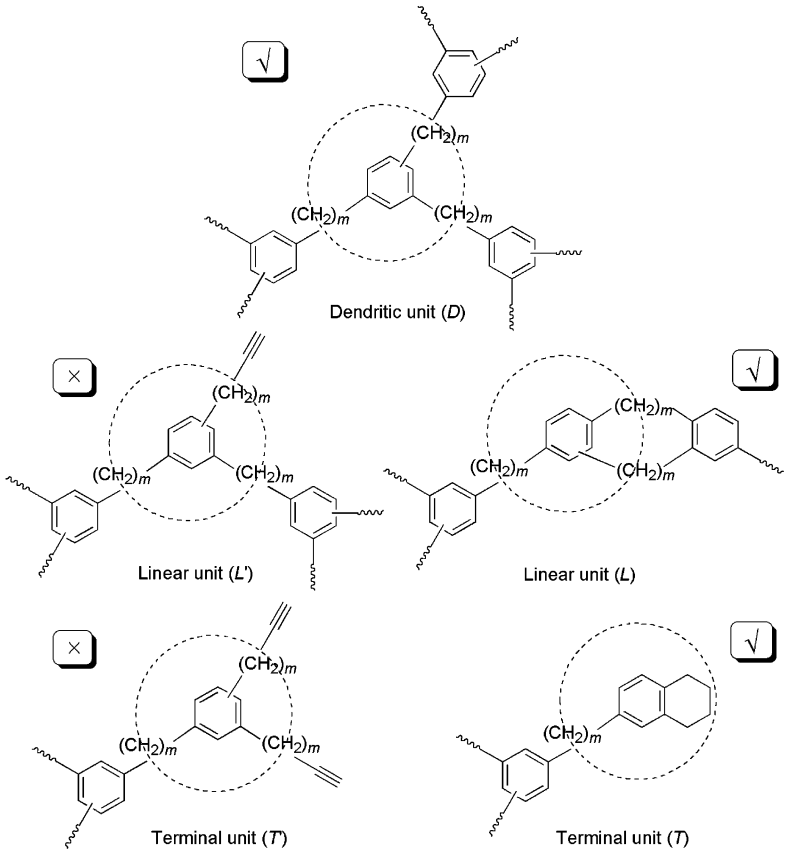

detected any absorption peaks associated with the resonance of the ethynyl groups. Such triple bonds thus must have been consumed by their dimerization reactions with the diyne molecules, as exemplified in Scheme 6 for the case of polycyclotrimerization of **1**(4). When a pure linear chain [**4**(4)] is terminated by the dimerization end-capping reactions, a linear polymer [*l*-P**1**(4)] will be resulted. In this extreme case, the molar ratio of the terminal groups to the repeat units is virtually 0 when the degree of polymerization or the molecular weight of the polymer becomes high enough.[27] On the other hand, when a pure dendritic sphere [**6**(4)] is end-capped by the dimerization reactions, a dendritic polymer [*d*-P**1**(4)] will be formed. In this extreme case, the molar ratio of the terminal groups to the repeat units rapidly approaches to 1 with an increase in the number of generations.[10,28]

The real situation is in between these two extreme cases. As discussed above (cf. Figure 7 and eq 3), the experimental value for the molar ratio of cyclic to acyclic units ($R_{C/A}$) is 48%. Let us examine what kinds of cyclic and acyclic units exist in the polymer. Theoretically there are five such structures: one dendritic unit (*D*), two liner units (*L*′ and *L*), and two terminal units (*T*′ and *T*), as illustrated in Chart 3. The spectroscopic analyses have, however, found no triple bonds in the polymer—the existence of units *L*′ and *T*′ can thus be ruled out. Among the three units left, *T* is a cyclic structure and *D* and *L* are acyclic ones.[29] The molar ratio of cyclic *T* unit to acyclic *D* and *L* units thus should be equal to $R_{C/A}$, viz., 0.48. This value is between 0 (exclusive linear growth) and 1 (exclusive dendritic growth), indicating that the alkyne polycyclotrimerization has proceeded in both linear and dendritic propagation modes. The simultaneous linear and dendritic propagations lead to the formation of a hyperbranched polymer with a glycogen-like molecular structure, consisting of the repeat units of acyclic linear chains (*L*)

Table 4. Ideal Growth Patterns of Dendritic and Terminal Units in Diyne Polycyclotrimerization[a]

		(N_D', N_T')						
no.	L	G_1	G_2	G_3	G_4	G_5	···	G_x
1	L_0	(1, 3)	(4, 6)	(10, 12)	(22, 24)	(46, 48)	···	$(3 \times 2^{x-1} - 2, 3 \times 2^{x-1})$
2	L_1		(1, 3)	(7, 9)	(19, 21)	(43, 45)	···	$(3 \times 2^{x-1} - 2 - 3, 3 \times 2^{x-1} - 3)$
3	L_2			(4, 6)	(16, 18)	(40, 42)	···	$(3 \times 2^{x-1} - 2 - 6, 3 \times 2^{x-1} - 6)$
4	L_3			(1, 3)	(13, 15)	(37, 39)	···	$(3 \times 2^{x-1} - 2 - 9, 3 \times 2^{x-1} - 9)$
5	L_4				(10, 12)	(34, 36)	···	$(3 \times 2^{x-1} - 2 - 12, 3 \times 2^{x-1} - 12)$
6	L_5				(7, 9)	(31, 33)	···	$(3 \times 2^{x-1} - 2 - 15, 3 \times 2^{x-1} - 15)$
7	···				···	···	···	···
8	L_y							$(3 \times 2^{x-1} - 2 - 3y, 3 \times 2^{x-1} - 3y)$

[a] Abbreviations: L = number of linear growths, G = number of generations, N_D' = number of dendritic units in the ideal model, and N_T' = number of terminal units in the ideal model.

Scheme 7

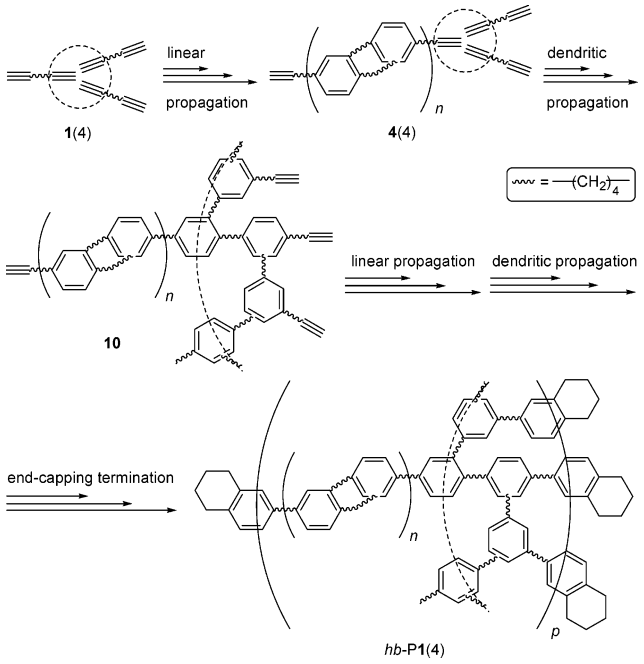

and dendritic branches (*D*), with all their ends capped by cyclic terminal units (*T*; Scheme 7).

The degree of branching (DB) is an important structural parameter for a hyperbranched polymer. It is, however, difficult to directly measure the DB of *hb*-P**1**(4) because the spectrometers cannot differentiate its *L* and *D* units.[29] This technical difficulty forces us to take a different approach, and ideal models are thus built in an effort to deduce the necessary equations for calculating the DB value. Assuming that the propagating species grow in an ideal dendritic mode with their peripheral triple bonds all end-capped by the tetralin-type cyclic terminal units, perfect dendrimers with globular geostructures will be generated. A few examples of such ideal dendrimers with generation numbers 1−3 (or G_1−G_3) are given in the first row of Chart 4 [noting that no linear growth is involved in this specific case; thus, all the dendrimers possesses 0 linear unit (L_0)]. The sequential growth patterns of the *D* and *T* units in the ideal dendrimers are given in Table 4 (no. 1), which shows clearly that with an increase in the number of generation (x) the numbers of *D* (N_D') and *T* units (N_T') increase, and their ratio ($R_{T/D}'$) rapidly approaches 1 (eq 4).

$$R_{T/D}' = \lim_{x\to\infty} \frac{N_T'}{N_D'} = \lim_{x\to\infty} \frac{3 \times 2^{x-1}}{3 \times 2^{x-1} - 2} = 1 \qquad (4)$$

If the linear propagation mode participates, the geostructures of the resultant polymers will vary (Chart 4) and their N_D' and N_T' values will decrease with an increase in the number of linear growths (y), when compared to those of their counterparts of ideal dendrimers with the same generation numbers (Table 4). Whereas both N_T' and N_D' change with y, their ratio $R_{T/D}'$ remains almost constant. Indeed, when x is high enough, $R_{T/D}'$ approaches unity, viz., $N_T' = N_D'$. This can be readily appreciated by comparing the general formulas given in the last column of Table 4: when x is large enough, the difference between N_T' $(3 \times 2^{x-1} - 3y)$ and N_D' $(3 \times 2^{x-1} - 2 - 3y)$ is marginally small. This can also be easily understood by looking over the example of propagation reaction given in Scheme 8. When a propagating species (**11**) with a high x value and a unity $R_{T/D}$ ratio undergoes a series of liner growths, a new propagating species (**14**) is formed. During the linear growths, the N_D and N_T values experience little change. The following relationship thus holds in the diyne polycyclotrimerization, regardless whether there are any linear units in the polymer structure:

$$N_T = N_D (x \to \infty) \qquad (5)$$

As discussed above, in the real case of the diyne polycyclotrimerization, there are one type of cyclic terminal unit (*T*) and two types of acyclic repeat units (*D* and *T*; cf. Chart 3). Equation 3 can thus be changed to eq 6, where N_L is the number of linear units:

$$R_{C/A} = \frac{N_T}{N_D + N_L} = \frac{3A_e}{2A_f - A_e} = 0.48 \qquad (6)$$

When N is used to represent the number of all structural units in the polymer, the following equation holds by definition:

$$N_D + N_L + N_T = N \qquad (7)$$

Dividing eqs 5−7 by N gives the following equations:

$$f_T = f_D \qquad (8)$$

$$\frac{f_T}{f_D + f_L} = 0.48 \qquad (9)$$

$$f_D + f_L + f_T = 1 \qquad (10)$$

where f_T, f_D, and f_L are the molar fractions of terminal (N_T/N), dendritic (N_D/N), and linear units (N_L/N), respectively. From eqs 8−10, f_T, f_D, and f_L are determined

Chart 4

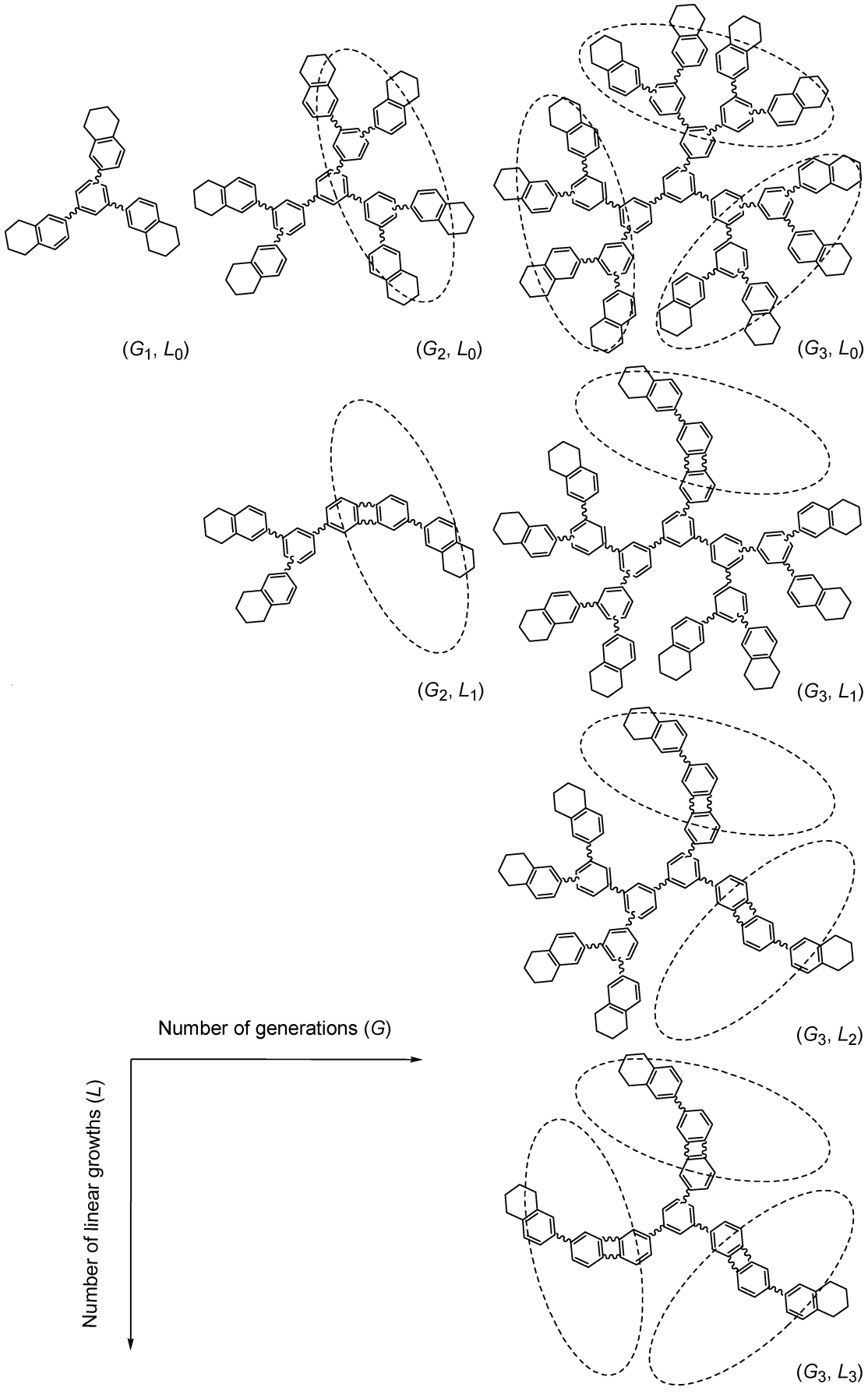
(G_1, L_0)
(G_2, L_0)
(G_3, L_0)
(G_2, L_1)
(G_3, L_1)
(G_3, L_2)
(G_3, L_3)
Number of generations (G)
Number of linear growths (L)

Scheme 8

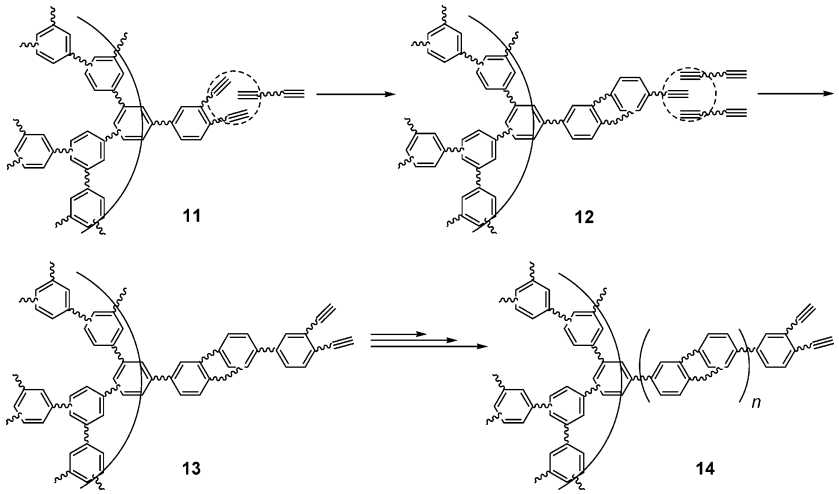

by simple calculations to be 32%, 32%, and 36%, respectively.

For a hyperbranched polymer prepared from a polycondensation reaction of an AB_m-type monomer, its DB is defined by eq 11.[30] This equation can be rewritten as eq 12 by dividing its denominator and numerator by N:

$$\mathrm{DB} = \frac{N_\mathrm{D} + N_\mathrm{T}}{N_\mathrm{D} + N_\mathrm{L} + N_\mathrm{T}} \tag{11}$$

$$\mathrm{DB} = \frac{f_\mathrm{D} + f_\mathrm{T}}{f_\mathrm{D} + f_\mathrm{L} + f_\mathrm{T}} \tag{12}$$

Putting the f_D, f_L, and f_T values into eq 12 yields a DB value of 64%. This DB value, in addition to the firm spectroscopic analysis data, further confirms the hyperbranched nature of the molecular structure of our polymer.[30,31]

Concluding Remarks

In summary, in this work, we have synthesized a group of new hyperbranched poly(alkenephenylene)s by transition-metal-catalyzed alkyne polycyclotrimerizations. What we have achieved in this work can be summarized as follows:

(1) *Catalysts exploration*. Effective, single-component catalysts ($TaBr_5$, $NbBr_5$, and $NbBr_3$·DME) for alkyne polycyclotrimerization are developed. These catalysts enjoy such advantages as high activity and operational simplicity as well as commercial availability and low costs. The excellent performance of $NbBr_3$·DME in the diyne polycyclotrimerization suggests the possibility of exploring new catalysts with even higher activity from the organometallic complexes by tuning molecular structures of their ligands, which is currently pursued in our laboratories.

(2) *Polymerization control*. Alkyne polycyclotrimerization is in some sense a difficult reaction, which often runs out of control to give cross-linked polymers of intractability.[10−12] The effects of the reaction parameters including $[M]_0$, [cat.], solvent, time, and temperature are systematically investigated in this work, and under optimal reaction conditions, high molecular weight polymers (with M_w up to $\sim 270 \times 10^3$) are reproducibly prepared in high yields (normally >80%), which are completely soluble and readily processable.

(3) *Structural determination*. The spectra of the polymers seemed simple at first glance but troubled us when we scrutinized the details. The most confusing result was the complete absence of triple-bond resonance in the spectra because a hyperbranched polymer prepared from alkyne polycyclotrimerization was expected to carry many triple bonds on its peripheral surface. With the aid of the model reactions, the spectra are fully elucidated, from which the structures and ratios of the *L*, *D*, and *T* units are determined and the hyperbranched nature of the polymer structure is confirmed.

(4) *Mechanistic understanding*. The structural analyses and the model simulations enable mechanistic deciphering. The propagations in the diyne polycyclotrimerization share some similarity to glycogenesis: the active centers simultaneously grow in *L* and *D* modes, giving the *L* and *D* units, respectively. [It is the *L* growth that has considerably decreased the number of *T* units (by ∼50 mol % from that obtainable from the pure *D* growth).] The triple bonds at the ends of the *L* chains and on the peripheries of the *D* spheres are all consumed by their dimerizations with the alkyne monomers, yielding the tetralin-type *T* units. The end-capping reaction is so beautifully done that no triple-bond moieties in the polymer structures can be detected by all the spectrometers we employed for the structural analyses.

(5) *Property discovery*. The new polymers are expected to exhibit many interesting properties, and in this study, their unique, useful thermal properties are uncovered. Polymer *hb*-P**1**(4) can be readily cured at moderate temperatures (e.g., ∼100 °C) and lose almost no weight at high temperatures (up to ∼500 °C). Similarly, no weight losses are observed when its structural congeners, i.e., *hb*-P**1**(5) and *hb*-P**1**(6), are heated to comparably high temperatures. The polymers containing silicon and nitrogen heteroatoms exhibit even more impressive thermal behaviors: they graphitize or ceramize in high yields (up to 80%) when pyrolyzed at 900 °C in an inert atmosphere.[17] These outstanding thermal properties may enable the polymers to find high-tech applications as, e.g., solvent- and moisture-resistant coatings, thermally and dimensionally stable films, and processable precursors to nanostructured materials such as carbon nanotubes[32,33] and SiC ceramics.[34,35]

Acknowledgment. The work described in this paper was partially supported by the Research Grants Council (Projects N_HKUSR606_03, 604903, HKUST6085/02P, and 6121/01P) and the University Grants Committee of Hong Kong through an Area of Excellence Scheme (Project AoE/P-10/01-1A).

Supporting Information Available: IR spectra of **1**(4) and *hb*-P**1**(4) and UV absorption spectra of DCM solutions of *hb*-P**1**(4), **8**, and **1**(4). This material is available free of charge via the Internet at http://pubs.acs.org.

References and Notes

(1) *Biopolymers from Polysaccharides and Agroproteins*; Gross, R. A., Scholz, C., Eds.; American Chemical Society: Washington, DC, 2001.

(2) Small saccharides other than glucose can also form hyperbranched biopolymers. Galactose, for example, can be polymerized into galactogen, a polysaccharide with a branched molecular structure similar to that of glycogen.

(3) Teusink, B.; Passarge, J.; Reijenga, C. A.; Esgalhado, E.; van der Weijden, C. C.; Schepper, M.; Walsh, M. C.; Bakker, B. M.; van Dam, K.; Westerhoff, H. V.; Snoep, J. L. *Eur. J. Biochem.* **2000**, *267*, 5313−5329.

(4) (a) Saier, M. H. *Mechanisms and Regulation of Carbohydrate Transport in Bacteria*; Academic Press: Orlando, FL, 1985. (b) Shimeno, S. *Studies on Carbohydrate Metabolism in Fish*; A.A. Balkema: Rotterdam, 1982. (c) *Carbohydrate Reserves in Plants: Synthesis and Regulation*; Gupta, A. K., Kaur, N., Eds.; Elsevier: New York, 2000.

(5) Amylopectin, a hyperbranched biopolymer of glucose in plants, is less branched than glycogen, probably because the energy storage and transport in plants are less demanding in speed than those in animals, taking into consideration that the living machineries in plants experience less vigorous changes than those in animals.[1,4]

(6) (a) *Dendrimers V: Functional and Hyperbranched Building Blocks, Photophysical Properties, Applications in Materials and Life Sciences*; Schalley, C. A., Vogtle, F., Eds.; Springer-Verlag: Berlin, 2003. (b) *Dendrimers and Other Dendritic Polymers*; Frechet, J. M. J., Tomalia, D. A., Eds.; Wiley: New York, 2002.

(7) (a) Zhao, D. H.; Moore, J. S. *Chem. Commun.* **2003**, 807−818. (b) Tomalia, D. A.; Frechet, J. M. J. *J. Polym. Sci., Part A: Polym. Chem.* **2002**, *40*, 2719−2728. (c) Crooks, R. M. *Chem. Phys. Chem.* **2001**, *2*, 644−654. (d) Watson, M. D.; Fechtenkotter, A.; Mullen, K. *Chem. Rev.* **2001**, *101*, 1267−1300. (e) Jikei, M.; Kakimoto, M. *Prog. Polym. Sci.* **2001**, *26*, 1233−1285. (f) Voit, B. *J. Polym. Sci., Part A: Polym. Chem.* **2000**, *38*, 2505−2525. (g) Frey, H.; Schlenk, C. *Top. Curr. Chem.* **2000**, *210*, 69−129. (h) Siemsen, P.; Livingston, R. C.; Diederich, F. *Angew. Chem., Int. Ed.* **2000**, *39*, 2633−2657. (i) Bunz, U. H. F. *Chem. Rev.* **2000**, *100*, 1605−1644. (j) Hult, A.; Johansson, M.; Malmstrom, E. *Adv. Polym. Sci.* **1999**, *143*, 1−34. (k) Scherf, U. *Top. Curr. Chem.* **1999**, *201*, 163−222. (l) Hawker, C. J. *Curr. Opin. Colloid Interface Sci.* **1999**, *4*, 117−121. (m) Newkome, G. R.; He, E. F.; Moorefield, C. N. *Chem. Rev.* **1999**, *99*, 1689−1746. (n) Bosman, A. W.; Janssen, H. M.; Meijer, E. W. *Chem. Rev.* **1999**, *99*, 1655−1688. (o) Kim, Y. H. *J. Polym. Sci., Part A: Polym. Chem.* **1998**, *36*, 1685−1698.

(8) (a) Miller, T. M.; Neenan, T. X.; Zayas, R.; Bair, H. E. *J. Am. Chem. Soc.* **1992**, *114*, 1018−1025. (b) Tour, J. M. *Adv. Mater.* **1994**, *6*, 190−198. (c) Johnen, N. A.; Kim, H. K.; Ober, C. K. *ACS Symp. Ser.* **1994**, *579*, 298−315. (d) Hecht, S.; Frechet, J. M. J. *J. Am. Chem. Soc.* **1999**, *121*, 4084−4085. (e) Mitsutoshi, J.; Ken, F.; Yang, G.; Kakimoto, M. *Macromolecules* **2000**, *33*, 6228−6234. (f) Cameron, C.; Fawcett, A. H.; Hetherington, C. R.; Mee, R. A. W.; McBride, F. V. *Macromolecules* **2000**, *33*, 6551−6568. (g) Weil, T.; Wiesler, U.-M.; Herrmann, A.; Bauer, R.; Hofkens, J.; De Schryver, F. C.; Mullen, K. *J. Am. Chem. Soc.* **2001**, *123*, 8101−8108. (h) Komber, H.; Ziemer, A.; Voit, B. *Macromolecules* **2002**, *35*, 3514−3519. (i) Markoski, L. J.; Thompson, J. L.; Moore, J. S. *Macromolecules* **2002**, *35*, 1599−1603.

(9) (a) Zheng, R.; Lam, J. W. Y.; Peng, H.; Häussler, M.; Tang, B. Z. *Polym. Mater. Sci. Eng.* **2003**, *89*, 442−443. (b) Zheng, R.; Lam, J. W. Y.; Peng, H.; Häussler, M.; Law, C. C. W.; Tang, B. Z. *Polym. Prepr.* **2003**, *44* (2), 770−771.

(10) (a) Chen, J.; Peng, H.; Law, C. C. W.; Dong, Y.; Lam, J. W. Y.; Williams, I. D.; Tang, B. Z. *Macromolecules* **2003**, *36*, 4319−4327. (b) Xu, K.; Peng, H.; Sun, Q.; Dong, Y.; Salhi, F.; Luo, J.; Chen, J.; Huang, Y.; Zhang, D.; Xu, Z.; Tang, B. Z. *Macromolecules* **2002**, *35*, 5821−5834. (c) Peng, H.; Cheng, L.; Luo, J.; Xu, K.; Sun, Q.; Dong, Y.; Salhi, F.; Lee, P. P. S.; Chen, J.; Tang, B. Z. *Macromolecules* **2002**, *35*, 5349−5351. (d) Peng, H.; Luo, J.; Cheng, L.; Lam, J. W. Y.; Xu, K.; Dong, Y.; Zhang, D.; Huang, Y.; Xu, Z.; Tang, B. Z. *Opt. Mater.* **2002**, *21*, 315−320. (e) Xu, K.; Tang, B. Z. *Chin. J. Polym. Sci.* **1999**, *17*, 397−402.

(11) (a) Mi, Y.; Tang, B. Z. *Polym. News* **2001**, *26*, 170−176. (b) Lam, J. W. Y.; Luo, J.; Peng, H.; Xie, Z.; Xu, K.; Dong, Y.; Cheng, L.; Qiu, C.; Kwok, H. S.; Tang, B. Z. *Chin. J. Polym. Sci.* **2001**, *19*, 585−590. (c) Lam, J. W. Y.; Chen, J.; Law, C. C. W.; Peng, H.; Xie, Z.; Cheuk, K. K. L.; Kwok, H. S.; Tang, B. Z. *Macromol. Symp.* **2003**, *196*, 289−300. (d) Xie, Z.; Peng, H.; Lam, J. W. Y.; Chen, J.; Zheng, Y.; Qiu, C.; Kwok, H. S.; Tang, B. Z. *Macromol. Symp.* **2003**, *195*, 179−184. (e) Häussler, M.; Lam, J. W. Y.; Zheng, R.; Peng, H.; Luo, J.; Chen, J.; Law, C. C. W.; Tang, B. Z. *C. R. Chim.* **2003**, *6*, 833−842.

(12) Xu, K. Ph.D. Dissertation, Hong Kong University of Science & Technology, Dec 2000.

(13) (a) Muchtar, Z.; Schappacher, M.; Deffieux, A. *Macromolecules* **2001**, *34*, 7595. (b) Grayson, S. M.; Frechet, J. M. J. *Macromolecules* **2001**, *34*, 6542. (c) Uhrich, K. E.; Hawker, C. J.; Frechet, J. M. J.; Turner, S. R. *Macromolecules* **1992**, *25*, 4583.

(14) Zheng, R.; Peng, H.; Lam, J. W. Y.; Chen, J.; Häussler, M.; Tang, B. Z. *Polym. Prepr.* **2003**, *44* (1), 956−957.

(15) (a) Xu, K.; Peng, H.; Lam, J. W. Y.; Poon, T. W. H.; Dong, Y.; Xu, H.; Sun, Q.; Cheuk, K. K. L.; Salhi, F.; Lee, P. P. S.; Tang, B. Z. *Macromolecules* **2000**, *33*, 6918−6924. (b) Tang, B. Z.; Xu, K.; Sun, Q.; Lee, P. P. S.; Peng, H.; Salhi, F.; Dong, Y. *ACS Symp. Ser.* **2000**, *760*, 146−164. (c) Tang, B. Z.; Poon, W. H.; Leung, S. M.; Leung, W. H.; Peng, H. *Macromolecules* **1997**, *30*, 2209−2212. (d) Tang, B. Z.; Kotera, N. *Macromolecules* **1989**, *22*, 4388−4390.

(16) Lam, J. W. Y.; Tang, B. Z. *J. Polym. Sci., Part A: Polym. Chem.* **2003**, *41*, 2607−2629.

(17) (a) Preliminary results have been reported in ref 9b. (b) Zheng, R.; Dong, H.; Lam, J. W. Y.; Tang, B. Z. Manuscript in preparation.

(18) (a) *Handbook of Metathesis*; Grubbs, R. H., Ed.; Wiley-VCH: Weinheim, 2003. (b) Choi, S. K.; Gal, Y. S.; Jin, S. H.; Kim, H. K. *Chem. Rev.* **2000**, *100*, 1645−1681. (c) *Metathesis Polymerization of Olefins and Polymerization of Alkynes*; Imamoglu, Y., Ed.; Kluwer: Boston, 1998. (d) Ivin, K. J.; Mol, J. C. *Olefin Metathesis and Metathesis Polymerization*; Academic Press: San Diego, 1997. (e) Ginsburg, E. J.; Gorman, C. B.; Grubbs, R. H. In *Modern Acetylene Chemistry*; Stang, P. J., Diederich, F., Eds.; VCH: Weinheim, 1995; Chapter 10. (f) Shirakawa, H.; Masuda, T.; Takeda, K. In *The Chemistry of Triple-Bonded Functional Groups*, Supplement C2; Patai, S., Ed.; Wiley: New York, 1994; Chapter 17.

(19) (a) Lam, J. W. Y.; Dong, Y.; Cheuk, K. K. L.; Luo, J.; Xie, Z.; Kwok, H. S.; Mo, Z.; Tang, B. Z. *Macromolecules* **2002**, *35*, 1229−1240. (b) Tang, B. Z.; Xu, H.; Lam, J. W. Y.; Lee, P. P. S.; Xu, K.; Sun, Q.; Cheuk, K. K. L. *Chem. Mater.* **2000**, *12*, 1446−1455. (c) Huang, Y. M.; Lam, J. W. Y.; Cheuk, K. K. L.; Ge, W.; Tang, B. Z. *Macromolecules* **1999**, *32*, 5976−5978. (d) Tang, B. Z.; Kong, X.; Wan, X.; Peng, H.; Lam, W. Y.; Feng, X.; Kwok, H. S. *Macromolecules* **1998**, *31*, 2419−2432.

(20) (a) Silverstein, R. M.; Webster, F. X. *Spectrometric Identification of Organic Compounds*, 6th ed.; Wiley: New York, 1998. (b) Pretsch, E.; Buhlmann, P.; Affolter, C. *Structure Determination of Organic Compounds: Tables of Spectral Data*, 3rd ed.; Springer: Berlin, 2000. (c) Field, L. D.; Sternhell, S.; Kalman, J. R. *Organic Structures from Spectra*, 3rd ed.; Wiley: New York, 2002.

(21) Masuda, T.; Tang, B. Z.; Higashimura, T.; Yamaoka, H. *Macromolecules* **1985**, *18*, 2369−2373.

(22) Goosy, M. In *Specialty Polymers*; Dyson, R. W., Ed.; Blackie: London, 1987; Chapter 5, pp 83−109.

(23) (a) Saito, S.; Yamamoto, Y. *Chem. Rev.* **2000**, *100*, 2901−2915. (b) Lautens, M.; Klute, W.; Tam, W. *Chem. Rev.* **1996**, *96*, 49−92. (c) Schore, N. E. *Chem. Rev.* **1988**, *88*, 1081−1119. (d) Vollhardt, K. P. C. *Angew. Chem., Int. Ed. Engl.* **1984**, *23*, 539−644. (e) Maitlis, P. M. *Acc. Chem. Res.* **1976**, *9*, 93−99.

(24) (a) Cotton, F. A.; Hall, W. T. *J. Am. Chem. Soc.* **1979**, *101*, 5094−5095. (b) Bruck, M. A.; Copenhaver, A. S.; Wigley, D.

E. *J. Am. Chem. Soc.* **1987**, *109*, 6525−6527. (c) Strickler, J. R.; Wexler, P. A.; Wigley, D. E. *Organometallics* **1988**, *7*, 2067−2069. (d) Bianchini, C.; Caulton, K. G.; Chardon, C.; Eisenstein, O.; Folting, K.; Johnson, T. J.; Meli, A.; Peruzzini, M.; Rauscher, D. J.; Streib, W. E.; Vizza, F. *J. Am. Chem. Soc.* **1991**, *113*, 5127−5129. (e) Strickler, J. R.; Wexler, P. A.; Wigley, D. E. *Organometallics* **1991**, *10*, 118−127. (f) Kwon, D.; Real, J.; Curtis, M. D.; Rheingold, A.; Haggerty, B. S. *Organometallics* **1991**, *10*, 143−148. (g) Pope, R. M.; Vanorden, S. L.; Cooper, B. T.; Buckner, S. W. *Organometallics* **1992**, *11*, 2001−2003. (h) Pelissier, H.; Rodriguez, J.; Vollhardt, K. P. C. *Chem.−Eur. J.* **1999**, *5*, 3549−3561.

(25) (a) Pouchert, C. J.; Behnke, J. *The Aldrich Library of ^{13}C and ^{1}H FT NMR Spectra*; Aldrich Chemical Co., Ltd.: Milwaukee, WI, 1993. (b) Feinstein, K. *Guide to Spectroscopic Identification of Organic Compounds*; CRC Press: Boca Raton, FL, 1995.

(26) (a) Matsuzaki, K.; Uryu, T.; Asakura, T. *NMR Spectroscopy and Stereoregularity of Polymers*; Japan Scientific Societies Press: Tokyo, 1996. (b) Bovey, F. A.; Mirau, P. A. *NMR of Polymers*; Academic Press: San Diego, CA, 1996. (c) *NMR Spectroscopy of Polymers in Solution and in the Solid State*; Cheng, H. N., English, A. D., Eds.; American Chemical Society: Washington, DC, 2003.

(27) (a) Carraher, C. E., Jr. *Seymour/Carraher's Polymer Chemistry*, 6th ed.; M. Dekker: New York, 2003. (b) Stevens, M. P. *Polymer Chemistry: an Introduction*, 3rd ed.; Oxford University Press: New York, 1999.

(28) (a) Markoski, L. J.; Thompson, J. L.; Moore, J. S. *Macromolecules* **2002**, *35*, 1599−1603. (b) Hölter, D.; Burgath, A.; Frey, H. *Acta Polym.* **1997**, *48*, 30−35.

(29) Although *L* may also be viewed as a cyclic structure, the NMR spectrometry does not treat it as a cyclic unit but an acyclic one because the big ring (12-membered ring when $m = 4$) with little ring strain gives resonance signals identical to those of the open branch (*D*).[10,12,20,25] (Indeed, if *L* exhibited resonance peaks different from those of *D*, that would be very helpful because it would make the estimation of the *L*/*D* molar ratio a straightforward, easy job.)

(30) (a) Hawker, C. J.; Lee, R.; Fréchet, J. M. J. *J. Am. Chem. Soc.* **1991**, *113*, 4583−4588. (b) Frey, H.; Hölter, D. *Acta Polym.* **1999**, *50*, 67−76.

(31) (a) Wang, M.; Gan, D.; Wooley, K. L. *Macromolecules* **2001**, *34*, 3215−3223. (b) Parker, D.; Feast, W. J. *Macromolecules* **2001**, *34*, 2048−2059. (c) Thompson, D. S.; Markoski, L. J.; Moore, J. S.; Sendijarevic, I.; Lee, A.; McHugh, A. J. *Macromolecules* **2000**, *33*, 6412−6415. (d) Radke, W.; Litvinenko, G.; Muller, A. H. E. *Macromolecules* **1998**, *31*, 239−248. (e) Yan, D. Y.; Muller, A. H. E.; Matyjaszewski, K. *Macromolecules* **1997**, *30*, 7024−7033. (f) Kim, Y. H.; Webster, O. W. *Macromolecules* **1992**, *25*, 5561−5572.

(32) (a) Gherghel, L.; Kubel, C.; Lieser, G.; Rader, H. J.; Mullen, K. *J. Am. Chem. Soc.* **2002**, *124*, 13130−13138. (b) Dai, L. M.; Patil, A.; Gong, X. Y.; Guo, Z. X.; Liu, L. Q.; Liu, Y.; Zhu, D. B. *Chem. Phys. Chem.* **2003**, *4*, 1150−1169. (c) Park, C.; Yoon, J.; Thomas, E. L. *Polymer* **2003**, *44*, 6725−6760.

(33) Tang, B. Z.; Xu, H. *Macromolecules* **1999**, *32*, 2569−2576.

(34) (a) Simon, P. F. W.; Ulrich, R.; Spiess, H. W.; Wiesner, U. *Chem. Mater.* **2001**, *13*, 3464−3486. (b) Corriu, R. J. P. *Angew. Chem., Int. Ed.* **2000**, *39*, 1376−1398. (c) Interrante, L. V.; Liu, Q.; Rushkin, I.; Shen, Q. *Appl. Organomet. Chem.* **1996**, *10*, 1−10. (d) Birot, M.; Pillot, J. P.; Dunogues, J. *Chem. Rev.* **1995**, *95*, 1443−1477. (e) Seyferth, D. *Adv. Chem. Ser.* **1995**, *245*, 131−160.

(35) (a) Sun, Q. H.; Xu, K. T.; Peng, H.; Zheng, R. H.; Haussler, M.; Tang, B. Z. *Macromolecules* **2003**, *36*, 2309−2320. (b) Sun, Q.; Xu, K.; Lam, J. W. Y.; Cha, J. A. P.; Zhang, X.; Tang, B. Z. *Mater. Sci. Eng., C* **2001**, *16*, 107−112. (c) Sun, Q.; Lam, J. W. Y.; Xu, K.; Xu, H.; Cha, J. A. P.; Wong, P. C. L.; Wen, G.; Zhang, X.; Jing, X.; Wang, F.; Tang, B. Z. *Chem. Mater.* **2000**, *12*, 2617−2624.

MA049871+